CENTRAL ASIAN JOURNAL OF WATER RESEARCH (2024) 10(1): 91-114

https://doi.org/10.29258/CAJWR/2024-R1.v10-1/91-114.eng

Central Asian Journal of Water Research

High-resolution dynamic downscaling of historical and future climate projections over Central Asia

Erkin Isaev [a,d], Akihiko Murata [b], Shin Fukui [b], Roy C. Sidle [a,c]

[a] Mountain Societies Research Institute, University of Central Asia, Toktogul St., 138, Bishkek, 720001, Kyrgyz Republic
[b] Meteorological Research Institute, Japan Meteorological Agency, 1-1 Nagamine, Tsukuba, Ibaraki, 305-0052, Japan
[c] Tokyo University of Agriculture and Technology, Fuchu, 7293212, Japan
[d] Food and Agriculture Organization of the United Nations, Bangkok, 10700, Thailand

ABSTRACT

Climate change poses various challenges for agriculture and water management practices in Central Asia (CA). Central to these challenges are cryosphere dynamics, fragile mountain ecosystems, and ongoing natural hazards that highlight the need for robust projections of regional climate change. For the first time, dynamic downscaling was conducted in Central Asia at a spatial resolution of 5 km. This produced a regional dataset that incorporated periods between 1980 and 2000 and 2076 to 2096. Results show that dynamic downscaling significantly improves the simulation of temperature and precipitation across CA compared to General Circulation Models (GCMs) and other Regional Climate Models (RCMs) due to better representation of topography and related meteorological fields. Our analysis shows that there will be a significant warming trend in Central Asia with a projected increase of 6°C under the Shared Socioeconomic Pathway (SSP) scenario SSP5-8.5 from 2076 to 2096. Pronounced warming is detected over mountainous areas of CA from autumn to spring, which can be explained by the snow-albedo feedback. Precipitation increases are projected from winter to spring and decreases are projected from summer to autumn.

ARTICLE HISTORY

Received: August 16, 2023
Accepted: February 21, 2024
Published: March 5, 2024

KEYWORDS

Central Asia, dynamic downscaling, regional climate projections, high-resolution dataset

CONTACT Erkin Isaev erkiwa@gmail.com, University of Central Asia, Toktogul St., 138, Bishkek, 720001, Kyrgyz Republic

Published by Kazakh German University, Almaty/Kazakhstan

1. Introduction

The impacts of climate change increase challenges for agriculture and water management practices and adaptation in Central Asia (CA) (Immerzeel et al., 2010; Isaev, Kulikov, et al., 2022). Climate change alters the distribution of water resources across the region by changing seasonal precipitation and temperature patterns, and can significantly impact water resources (Gulakhmadov et al., 2020; Isaev, Ermanova, et al., 2022; Luo et al., 2018). While precipitation and temperature are critical elements of the water cycle (Chang et al., 2024; Ta et al., 2018; Wang et al., 2017), the frequent occurrence of extreme weather events, such as heatwaves, heavy rainfall, droughts, increasing temperature inversion days accompanied by air pollution, and biotic-abiotic catastrophes are evidence of climate change in this region (Alexander et al., 2006; Isaev, Ajikeev, et al., 2022; Isaev & Omurzakova, 2019; Kastridis et al., 2022; Pachauri, R.K., Meyer, 2014; Sillmann et al., 2013; Ta et al., 2018). Thus, current and future developments related to water and land use are significant national concerns and potential issues in international relations in the CA region (Bernauer & Siegfried, 2012). These issues highlight the need to evaluate the magnitude of changes in temperature and precipitation, both spatially and temporally (Wehner, 2013).

Mountainous regions of CA, mostly within Kyrgyzstan and Tajikistan, are among the top three most vulnerable countries to climate change in all of Eastern Europe and Central Asia (Manandhar et al., 2018). This vulnerability is largely attributable to climate-sensitive water and agricultural management systems and a lack of adaptive capacities in these areas (Kaplina et al., 2018). CA is threatened by glacier melting disrupting the water balance, which is affected by global warming (Park et al., 2021). Given the impacts of climate change on frequent natural hazards, strained water resources, and land degradation in CA, it is imperative to project regional climate change based on atmospheric emission scenarios to assess impacts, potential vulnerabilities, and adaptation strategies. Some climate projections have been conducted in CA using both regional (RCMs) and global (GCMs) climate models (Qiu et al., 2021). GCM simulations of precipitation across CA show mostly increases by the end of this century (Huang et al., 2014; Jiang et al., 2020). Studies estimate that the annual temperature in CA is rising faster than most other regions of the world (Muratalieva, 2022; Vakulchuk et al., 2022). However, GCMs typically have very coarse resolutions that cannot infer local scale climate of mountain topography where precipitation and temperature are greatly affected by complex terrain. Moreover, compared to GCMs, RCMs were essentially developed to downscale climate variables produced by coarse resolution GCMs, therefore providing data at a higher spatial resolution, more suitable for regional assessments of impacts, vulnerability, and

adaptation (Zhu et al., 2020). Generally, such a higher resolution leads to a better representation of finer-scale atmospheric and terrestrial processes (Rasmussen et al., 2011). Thus, it is common to downscale over regions of interest using RCMs (Bruyère et al., 2014). This strategy is essential for Kyrgyzstan, where more than 42% of the area is above 3000 m and more than 94% above 1000 m a.s.l. (Isaev, Ajikeev, et al., 2022); for Tajikistan more than 50% of the land is above 3000 m and more than 93% above 1000 m a.s.l. (Nowak et al., 2016).

Most of the previous RCM simulations across CA (Ozturk et al., 2017; Qiu et al., 2017, 2021; Russo et al., 2019, 2020; Wang et al., 2020; Zhu et al., 2020) used a single GCM from the Climate Model Intercomparison Project (CMIP) phase 5 as the boundary conditions, but in our research, for the first time in this region, lateral boundary conditions from MRI-AGCM3.2S were used (Mizuta et al., 2012). In MRI-AGCM3.2S the ensemble mean sea surface temperatures (SST) derived from future climate simulations with CMIP6 GCMs used for simulation by (Mizuta et al., 2012). Given the complex terrain in CA, GCM resolutions are low (≥ 20 km) and RCM simulation resolutions, although better, are rather low (9 km) for mountainous terrain (Qiu et al., 2021). Our dynamic downscaling study in CA is the first to employ a horizontal resolution of 5 km in this region.

The objective of this study is to highlight the importance of spatial resolution of the climate model across regions with complex orography by using data from Coordinated Regional Climate Downscaling Experiment (CORDEX) and CMIP6. In addition, because the focus of this investigation is to understand local climate and trends across CA and provide high-resolution climate data for environmental studies in the region, we used the regional model of the Meteorological Research Institute (MRI) of the Japan Meteorological Agency (JMA) named the non-hydrostatic regional climate model (NHRCM) (Sasaki et al., 2008) to produce high resolution climate information and future projections under high-end trajectories of climate futures (SSP5-8.5). Moreover, an important of this research is to inform CA agencies and municipalities related to preparation of long-term climate change adaptation and mitigation plans extending to the end of this century. Thus, we decided to produce climate projections for the period 2076-2096.

2. Methods and data

2.1. Regional model and experiment design

Here we used NHRCM for dynamical downscaling to simulate the regional climate over CA. NHRCM is a climate extension of JMA non-hydrostatic model (JMA-NHM), one of the numerical weather prediction models operated by JMA developed by (Saito et al., 2006, 2007). More detailed specifications of NHRCM are described in Murata et al., (2016, 2017).

The dynamic downscaling domain of NHRCM-CA (Fig. 1 b) incorporates 450 × 300 horizontal grid points with spacing of 5 km and 50 terrain-following vertical levels. The lowest level was 20 m above ground surface and the highest was 22 km. The study area covers mostly mountainous Central Asia, including the highest peaks, Ismoil Somoni (7495 m) and Victory Peak (7439 m) (Fig. 1 b). Long-term climate simulations use the following: (1) spectral nudging scheme (Nakano et al., 2012) based on spectral boundary coupling (Kida et al., 1991; Sasaki et al., 2000); (2) land-surface scheme developed by (Hirai & Oh'izumi, 2004; Yonehara et al., 2017) updated from (Oh'izumi, 2014); (3) Kain-Fritsch cumulus scheme (Kain & Fritsch, 1990); (4) cloud microphysics scheme (Lin & Farley, 1983); (5) Mellor-Yamada-Nakanishi-Niino level-2.5 boundary layer scheme (Nakanishi & Niino, 2004); (6) cloud radiation scheme (Kitagawa, 2000), and (7) clear-sky radiation scheme (Yabu et al., 2005).

Simulations for future climate were performed based on the SSP5-8.5 high-emission scenario because boundary conditions exist only for this scenario in MRI. The initial and boundary conditions were provided by an atmospheric general circulation model with a horizontal resolution of 20 km (MRI-AGCM3.2S) (Mizuta et al., 2012). For present and future regional climate simulations, the target periods are 20 years: the present simulation period spans September 1980 to August 2000, and the future simulation period spans September 2076 to August 2096; time integrations began on July 21 and ran through September 1 of the following year. To account for model spin-up, simulation results from the first 42 days were removed.

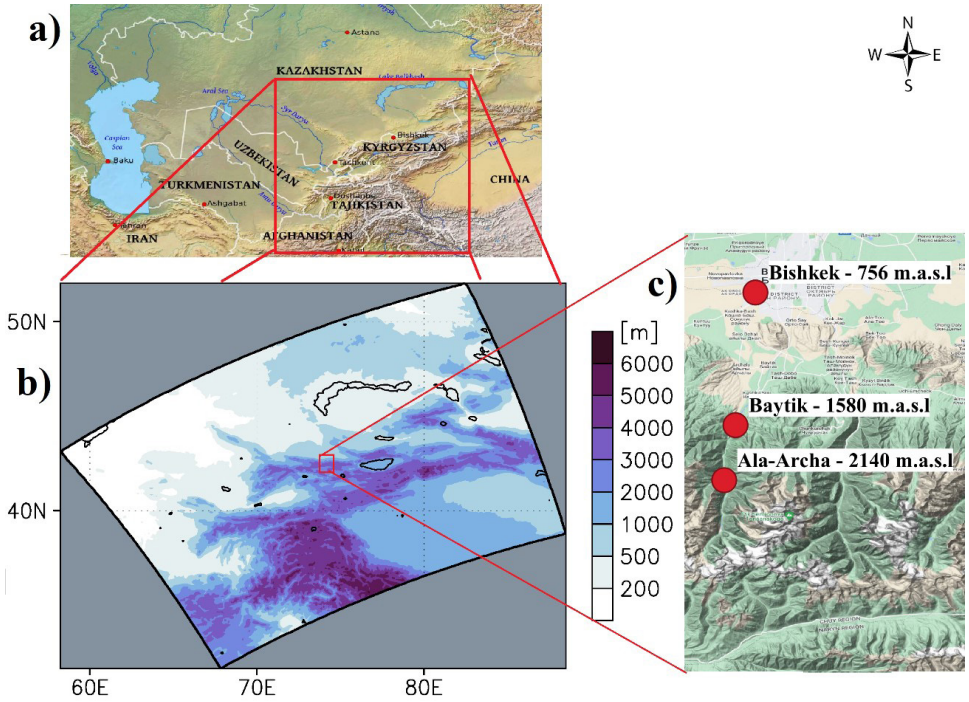

Figure 1. Study site: (a) Central Asia; (b) Downscaling domain; and (c) location of mountainous meteorological stations in the study site (Sources:(a) (Aitaliev et al., 2020), (b) model domain, (c) google terrain)

2.2. Data

The new generation of the Climatic Research Unit gridded Time Series Version 4 (CRU TS v4) with a spatial resolution of 0.5 x 0.5 degrees (Harris et al., 2020) is applied to evaluate the simulated temperature at annual and seasonal scales. Because only sparse and unevenly distributed rain gauge observations are merged in the gridded observations (e.g., CRU), new generation CHIRPS2.0 with a 5 km spatial resolution (Climate Hazards Group InfraRed Precipitation with Station data) (Funk et al., 2015) is used as "observations" for precipitation estimation. The main data sources used in the creation of CHIRPS2.0 were in situ precipitation observations obtained from a variety of sources including national meteorological services and remotely sensed data. For evaluation, the GCM (RCM) products are interpolated to the observations' grids using the bilinear (distance-weighted average) method.

As gridded observation data have potential limitations in depicting temperature and precipitation in mountainous region of CA, the model outputs were also evaluated with the meteorological station observations (Fig. 1c). We used monthly precipitation and monthly mean air temperature from meteorological stations in Bishkek, Baytik, and Ala-Archa (Fig. 1c) covering the period of 1980–2000. These observed climate data were taken from the Service on Hydrometeorology under the Ministry of Emergency Situations of the Kyrgyz Republic and Institute of Water Problems and Hydropower of the National Academy of Science of the Kyrgyz Republic (IWPH of the NAS KR).

Eleven CMIP6 GCMs were used in the comparison between the NHRCM-CA over mountainous CA, as previously recommended (Isaev, Ermanova, et al., 2022). Table I lists the GCMs and their basic descriptions. Six RCMs from the CAS-CORDEX regional experiment (Table I) were used in our research. Historical simulations of GCM monthly precipitation and surface air temperature were collected from data portals (CMIP5 Data Search | CMIP5 | ESGF-CoG, 2022; Cmip6 Data Search | Cmip6 | ESGF-CoG, 2022; CORDEX-DKRZ Data Search | CORDEX-DKRZ | ESGF-CoG, 2022).

Table I. Description of CMIP6 GCMs and CORDEX RCMs used in our study and their spatial resolution.

Institution, Country	CMIP6	Resolution, °	CAS-CORDEX	Resolution, °
Australian Research Council Centre of Excellence for Climate System Science, Australia	ACCESS-CM2	1.87 x 1.25	-	-
Beijing Climate Center, Beijing, China	BCC-CSM2-MR	1.12 × 1.12	-	-

Table I. Cont.

Institution, Country	CMIP6	Resolution, °	CAS-CORDEX	Resolution, °
Australian Research Council Centre of Excellence for Climate System Science, Australia	ACCESS-CM2	1.87 x 1.25	-	-
Beijing Climate Center, Beijing, China	BCC-CSM2-MR	1.12 × 1.12	-	-
Institute for Numerical Mathematics, Russia	INM-CM5-0	2.00 × 1.50	-	-
Institute Pierre Simon Laplace(IPSL), France	IPSL-CM6A-lR	2.50 × 1.27	-	-
Japan Agency for Marine-Earth Science and Technology (JAMSTEC), Japan	MIROC6	1.40 × 1.40	-	-
Max Planck Institute for Meteorology, Germany	MPI-ESM1-2-HR	0.94 × 0.94	RegCM4-3.v5	0.44 × 0.44
	MPI-ESM1-2-LR	1.87 × 1.86	REMO2015.v1	0.22 × 0.22
Meteorological Research Institute, Japan	MRI-ESM2-0	1.12 × 1.12	-	-
Norwegian Climate Centre, Norway	NorESM2-MM	1.00 × 1.00	REMO2015.v1	0.22 × 0.22
Met Office Hadley Centre, UK	HadGEM3-G	1.00 × 1.00	REMO2015.v1	0.22 × 0.22
	-	-	RegCM4-3.v5.	0.44 × 0.44
National Centre for Meteorological Research, France	CNRM-CM6-1	1.00 × 1.00	ALARO-0.v1	0.22 × 0.22
Meteorological Research Institute, Japan	MRI - AGCM3.2S	0.20 × 0.20		

2.3. Methods

Statistical analysis to compare model products with observations is necessary. The systematic error (BIAS) was used to evaluate model performance of climatological mean states. In addition, we used the ratio of standard deviation of simulations to that of observations (rSD). When rSD equals 1, simulation is optimal based on reproducing amplitudes of interannual variability.

To verify temperature simulations we adjusted simulated temperature, assuming a lapse rate of 0.0065 K m-1, to reduce elevation difference between the model grids and meteorological observation stations. Where simulated model grid temperature is added by multiplying with elevation difference between model grid and meteorological observation stations. Moreover, to calculate future temperature anomalies and the statistical significance of the changes, we used the bootstrap method, where future temperature and precipitation anomalies were estimated using 10,000 bootstrap samples with random replacement of 20-year dataset.

3. Results

3.1. Performance Evaluation of the NHRCM-CA

The BIAS pattern of temperature simulations from 1980 to 2000 (model minus observation) is close to that of precipitation simulations over Pamir-Alay and Tien-Shan mountains (Fig, 2). These similar BIAS patterns are because the CRU TS v4 and CHIRPS "observations" are limited in number across these regions. As such, gaps in CRU TS v4 and CHIRPS data can explain the large BIAS over these regions. The same large BIAS patterns were found in the previous research (Qiu et al., 2021; Zhu et al., 2020) over CA.

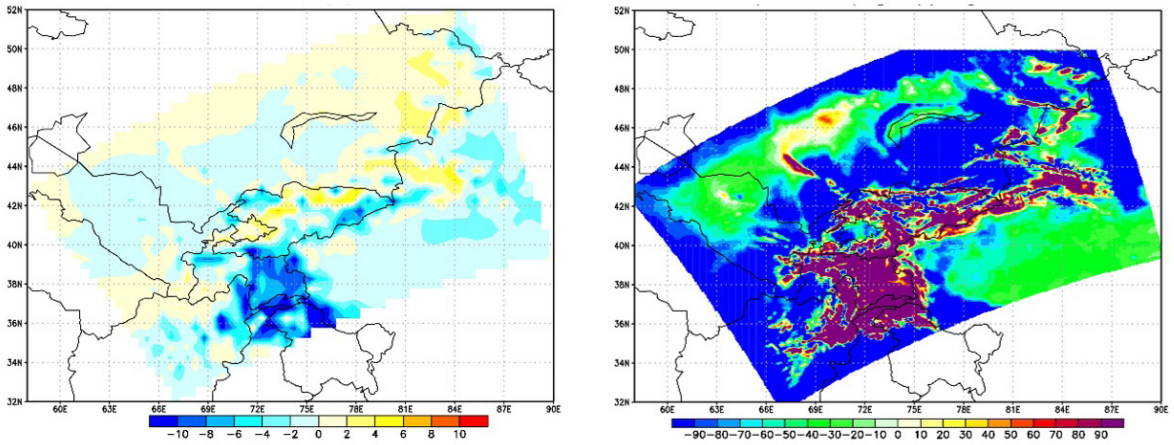

(a) (b)

Figure 2. BIAS of NHRCM-CA simulations for the period 1980-2000;
(a) BIAS of annual mean temperature, °C in year (NHRCM-CA minus CRU TS v4);
(b) BIAS of annual precipitation, mm in year (NHRCM-CA minus CHIRPS)

For seasonal simulations, the same BIAS patterns emerged for mean temperature with an average BIAS -6 oC (Fig. 3) and an average BIAS 80 mm/3 months for precipitation (Fig. 4) over Pamir-Alay and Tien-Shan mountains. Spring and summer

temperature simulations throughout CA were overestimated by about 2oC during three months (Fig. 3 c, b) and autumn and winter simulations were underestimated by about 2oC during three months (Fig. 3 a, d). The Pamir-Alay region is an exception, in which underestimation is observed in all seasons (approximately -7oC). In all seasons throughout mountainous CA, simulations overestimate precipitation, while in relatively flat and valley regions precipitation is underestimated (Fig. 4). Moreover, the errors in precipitation simulations are increasing towards the boundaries of the simulation domain.

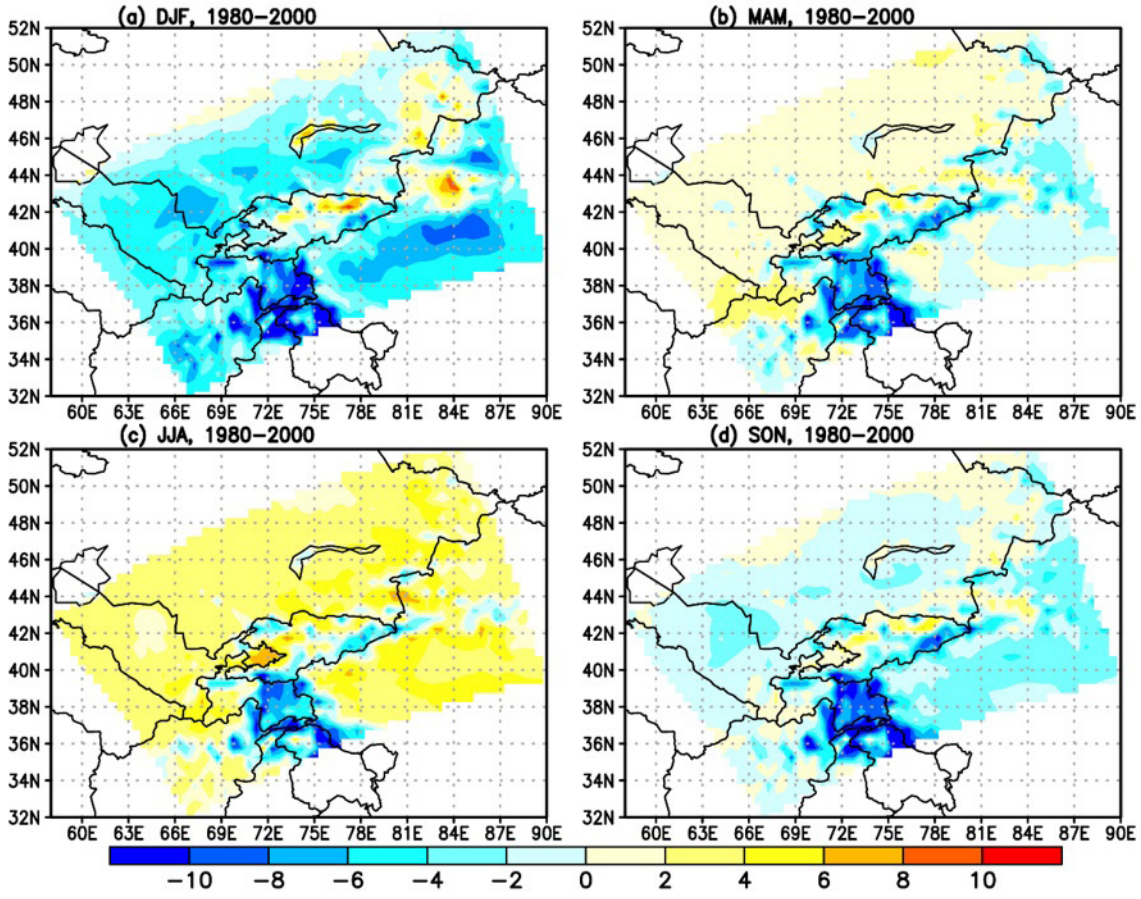

Figure 3. BIAS of seasonal mean temperature, oC (NHRCM-CA minus CRU TS v4) for the period 1980-2000: a) winter season; b) spring; c) summer; and d) autumn.

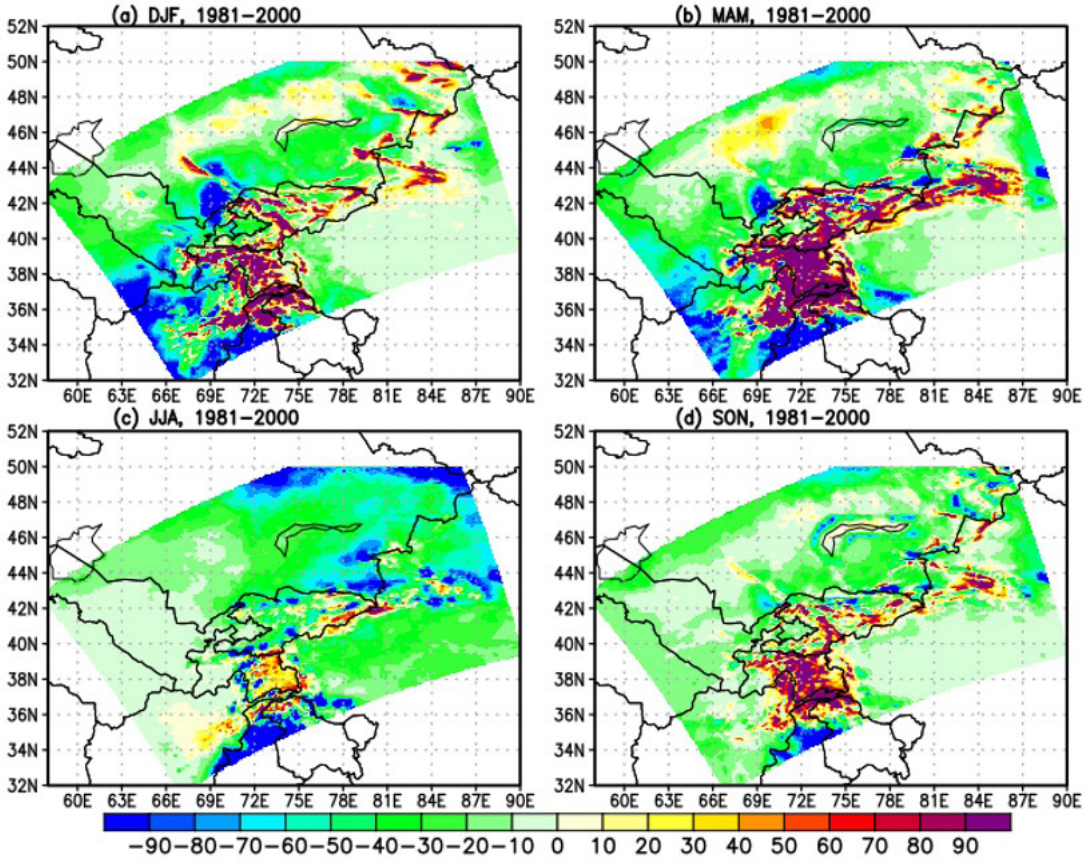

Figure 4. BIAS of seasonal precipitation, mm in 3 months (NHRCM-CA minus CHIRPS) for period 1980-2000: a) winter season; b) spring; c) summer; and d) autumn.

The performance of CMIP6 GCMs, CORDEX RCMs and NHRCM-CA RCM in reproducing monthly precipitation totals and monthly mean temperature for the period from 1980 to 2000 was assessed based on rSD metrics (Table II and III) with the best performance metrics (0.9 to 1.1) highlighted for the three stations. The grids with the smallest average absolute errors and significant correlation coefficients, calculated from the simulated 20-year mean monthly temperature and precipitation, were selected for verification from the nearest grids with a 5 km maximum radius from the weather stations, not the model grids proximate to the weather stations. Research on the validation of atmospheric models across mountainous regions (Isaev et al., 2017) shows that the environment of the observation station, such as topographic features, as well as the distances should be considered in selecting model grids.

Table II. Statistical summary of comparisons between the CORDEX RCMs, CMIP6 GCMs and NHRCM-CA monthly precipitation simulations and observations at Bishkek, Baytik, and Ala-Archa meteorological stations; rSD is the ratio between standard deviation of simulations and observations; MMEs are multi-model ensemble means; The best results are highlighted.

Meteorological stations	Temperature (rSD)																					
	Month	**ACCESS_CM2**	BCC_CSM2_MR	CNRM_CM6	HadGEM3_GC31_MM	INM_CM5.0	IPSL_CM6A_LR	MIROC6	MPI_ESM1_2-LR	MRI_ESM2-0	MPI-ESM1-2-HR	NorESM2-MM	ALARO-0.v1_CNRM	RegCm4-3v5-HadCEM2-ES	RegCm4-3v5-MPI-ESM-MR	**REMO2015_HadGEM2-ES**	REMO2015 MPI-M-ESM-LR	REMO2015 NCC-NorESM1-M	MRI-AGCM3.2S	**NHRCM-CA**	CMIP6 - MMEs	CAS-CORDEX-MMEs
Ala-Archa station, 2140 m.a.s.l.	1	1.2	1.7	3.1	1.6	1.4	3.4	2.5	1.5	2.5	2.2	1.7	1.5	2.4	3.6	**1.1**	1.6	2.2	1.4	**0.9**	2.1	2.1
	2	**1.1**	2.3	2.5	1.8	1.5	2.4	2.3	1.7	2.6	2.0	**0.9**	2.4	2.1	2.1	**1.1**	1.4	2.1	2.3	**1.1**	1.9	1.9
	3	0.7	**1.1**	1.5	**1.0**	0.8	1.4	**1.1**	1.5	1.5	1.4	0.6	1.6	1.4	1.6	1.2	**1.1**	**0.9**	2.2	**1.1**	1.2	1.3
	4	**1.0**	**1.0**	1.5	1.2	**1.1**	0.7	**1.0**	1.4	1.4	1.3	0.7	1.5	**1.1**	**1.1**	1.3	1.9	1.3	2.1	**0.9**	1.2	1.4
	5	**1.1**	1.2	1.2	1.3	**1.1**	0.6	**1.1**	1.4	1.2	1.2	**0.9**	1.7	1.5	1.3	1.2	**1.0**	0.8	2.8	**1.0**	**1.1**	1.3
	6	1.2	0.7	**1.1**	1.4	0.5	0.6	0.8	0.8	***1.1***	0.8	0.4	2.2	1.3	1.4	0.7	1.2	**1.0**	1.3	1.4	**0.9**	1.3
	7	0.8	0.4	**1.1**	1.2	0.6	**0.9**	0.6	0.2	1.2	0.2	0.5	3.1	1.3	**0.9**	0.6	**0.9**	0.7	**1.0**	0.5	0.7	1.3
	8	0.8	0.4	0.5	0.8	0.5	0.8	0.7	0.2	0.4	0.1	0.4	2.0	1.2	1.4	0.7	1.2	0.8	2.4	0.4	0.5	1.2
	9	1.2	0.7	1.6	1.5	0.5	**0.9**	0.8	0.5	0.8	0.8	0.4	2.7	1.3	2.2	1.3	1.9	1.4	1.6	**0.9**	**0.9**	1.8
	10	1.9	0.8	1.8	1.2	0.8	**1.1**	1.2	0.6	1.5	0.8	0.6	2.1	1.9	1.5	**1.0**	1.3	1.3	0.6	**0.9**	**1.1**	1.5
	11	1.6	0.8	1.9	1.7	**0.9**	1.4	**1.0**	1.2	1.4	1.9	**1.1**	0.8	2.7	2.2	**0.9**	2.2	1.2	0.7	**0.9**	1.4	1.7
	12	1.2	0.8	1.3	0.6	0.8	**1.1**	1.3	**0.9**	**1.1**	**1.1**	0.6	**0.9**	1.2	1.7	0.8	**1.0**	**1.1**	0.5	**0.9**	**1.0**	**1.1**
Baytik station, 1580 m.a.s.l.	1	**1.1**	1.5	2.8	1.5	1.3	3.1	2.3	1.4	2.3	2.0	1.6	1.3	2.2	3.3	1.5	2.8	2.0	1.3	**1.1**	1.9	2.2
	2	0.8	2.0	2.2	1.6	1.3	2.1	2.0	1.5	2.3	1.7	0.8	2.1	1.9	1.8	1.7	1.9	1.8	2.9	1.2	1.7	1.9
	3	0.6	**1.0**	1.3	**0.9**	0.8	1.2	**0.9**	1.3	1.3	1.2	0.5	1.3	1.2	1.4	1.8	**1.0**	0.8	1.9	**1.1**	**1.0**	1.3
	4	**0.9**	**0.9**	1.3	**1.1**	0.8	0.6	0.8	1.2	1.2	**1.1**	0.6	1.4	**1.0**	**1.0**	**1.1**	1.7	1.2	1.9	**1.0**	**1.0**	1.2
	5	**1.1**	1.2	1.2	1.3	**1.1**	0.6	**1.1**	1.4	1.2	1.2	**0.9**	1.7	1.5	1.3	1.2	**1.0**	0.8	2.8	**1.1**	1.1	1.3
	6	**1.1**	0.7	**1.0**	1.3	0.4	0.5	0.8	0.7	**1.0**	0.8	0.4	2.0	1.2	1.3	0.7	1.2	**0.9**	1.2	1.2	0.8	**1.2**
	7	0.7	0.3	**0.9**	**1.0**	0.4	0.7	0.5	0.2	**0.9**	0.1	0.4	2.4	**1.0**	0.7	0.5	0.7	0.5	0.7	0.3	0.6	1.0
	8	1.2	0.4	0.6	**1.0**	0.6	**1.0**	**0.9**	0.2	0.5	0.2	0.5	2.4	1.5	1.7	**0.9**	1.4	1.2	2.9	0.4	0.6	1.5
	9	**1.1**	0.6	1.4	1.4	0.5	0.8	0.7	0.4	0.7	0.7	0.4	2.4	1.2	1.9	**1.1**	1.7	1.2	1.4	**1.1**	0.8	1.6
	10	2.0	**0.9**	2.0	1.3	0.8	**1.1**	1.3	0.6	1.6	**0.9**	0.6	2.3	2.0	1.7	**1.0**	1.4	1.4	0.7	1.2	1.2	1.6
	11	1.8	0.8	2.1	1.9	**1.1**	1.5	**1.1**	1.3	1.6	2.2	1.3	**0.9**	3.0	2.4	1.4	2.5	1.3	**0.9**	**0.9**	1.5	1.9
	12	1.4	1.2	1.5	0.7	**1.0**	1.3	1.6	1.2	1.4	1.3	0.8	**1.1**	1.5	2.1	0.8	1.2	1.4	0.6	**0.9**	1.2	1.4
Bishkek station, 756 m.a.s.l.	1	0.7	**1.1**	2.0	1.2	**0.9**	2.2	1.6	**1.0**	1.6	1.3	**1.1**	1.6	1.4	2.3	**1.1**	1.8	1.5	1.5	**1.1**	1.3	1.6
	2	0.7	1.7	1.8	**1.0**	1.2	1.7	1.7	1.3	1.9	1.5	0.6	2.2	1.5	2.2	**1.1**	1.3	**1.1**	2.9	1.2	1.4	1.6
	3	0.7	**1.1**	1.4	**0.9**	0.8	1.3	**1.0**	1.4	1.4	1.3	0.5	1.8	1.2	**0.9**	**1.1**	0.8	0.8	1.9	**1.1**	**1.1**	**1.1**
	4	0.7	0.7	**1.1**	0.8	0.8	0.5	0.8	**1.0**	**1.0**	**1.0**	0.5	**1.1**	0.7	0.7	0.5	0.8	0.5	1.5	**0.9**	0.8	0.7
	5	1.3	1.2	1.3	1.6	1.3	0.8	1.3	1.6	1.4	1.7	**1.0**	1.6	1.5	**0.9**	0.8	0.8	0.7	**0.9**	**1.0**	1.3	**1.1**
	6	1.5	**0.9**	1.3	**1.0**	0.6	0.7	**1.1**	**0.9**	1.3	1.2	0.5	1.9	1.2	1.4	0.4	**1.0**	0.8	0.2	0.6	**1.0**	1.2
	7	**1.1**	0.5	1.4	**0.9**	0.7	**1.1**	0.8	0.2	1.5	0.5	0.6	2.2	**1.1**	1.6	0.3	0.7	0.5	0.3	0.2	0.8	**1.1**
	8	1.9	0.7	**0.9**	0.8	**0.9**	1.6	1.4	0.3	0.7	0.5	0.7	1.8	1.6	1.6	0.5	1.5	0.8	2.3	0.3	**0.9**	1.3
	9	1.4	0.8	1.8	0.6	0.6	1.2	0.8	0.5	**0.9**	0.8	0.4	1.9	**1.0**	1.5	0.6	**1.0**	0.7	2.1	**1.0**	0.8	1.1
	10	2.0	0.8	1.9	1.2	0.8	**1.1**	1.2	0.6	1.6	0.8	0.6	2.2	1.7	1.6	0.8	1.4	0.8	**1.1**	**1.0**	1.1	1.4
	11	1.4	0.7	1.6	**1.0**	0.8	1.2	0.8	**1.0**	1.2	1.4	**0.9**	**0.9**	2.1	1.3	**0.9**	1.7	**1.0**	**1.0**	**1.0**	**1.1**	1.3
	12	1.2	0.8	1.3	0.6	**0.9**	1.2	1.3	**1.0**	1.2	**1.1**	0.7	1.3	1.3	1.9	**0.9**	**1.0**	0.8	**0.9**	**0.9**	**1.0**	1.2

Table III. Statistical summary of the comparisons between the CORDEX RCMs, CMIP6 GCMs and NHRCM-CA monthly temperature simulations and observations at Bishkek, Baytik, and Ala-Archa meteorological stations; rSD is the ratio between standard deviation of simulations and observations; MMEs are multi-model ensemble means; The best results are highlighted.

Meteorological stations	Temperature (rSD)																					
	Month	**ACCESS_CM2**	BCC_CSM2_MR	CNRM_CM6	HadGEM3_GC31_MM	INM_CM5.0	IPSL_CM6A_LR	MIROC6	MPI_ESM1_2-LR	MRI_ESM2-0	MPI-ESM1-2-HR	NorESM2-MM	ALARO-0.v1_CNRM	RegCm4-3v5-HadCEM2-ES	RegCm4-3v5-MPI-ESM-MR	**REMO2015_HadGEM2-ES**	REMO2015 MPI-M-ESM-LR	REMO2015 NCC-NorESM1-M	MRI-AGCM3.2S	**NHRCM-CA**	CMIP6 - MMEs	CAS-CORDEX-MMEs
Ala-Archa station, 2140 m.a.s.l.	1	1.3	2.1	1.7	**1.0**	1.4	2.1	**1.0**	1.5	1.3	1.8	1.5	1.5	1.5	1.3	1.4	1.9	1.5	1.5	**0.9**	1.5	1.5
	2	**1.0**	1.3	**1.0**	0.8	**1.0**	1.5	**1.0**	**1.0**	0.8	**1.1**	**0.9**	1.2	0.8	1.2	0.7	1.3	1.3	**0.9**	**1.0**	**1.0**	1.2
	3	**1.1**	1.3	1.3	**1.1**	1.2	1.2	**1.0**	1.2	1.6	**1.1**	1.3	1.9	1.3	1.3	1.7	1.3	**1.1**	1.2	**1.1**	1.2	1.4
	4	**1.0**	1.4	1.2	1.2	0.8	1.3	0.8	**0.9**	**1.1**	1.2	**1.0**	**1.1**	**1.0**	**1.0**	1.2	1.2	0.8	0.5	**1.0**	**1.1**	**1.1**
	5	**1.1**	1.6	1.5	**1.0**	1.3	**1.1**	1.3	1.6	**1.1**	1.6	1.3	1.6	**0.9**	1.2	1.2	1.7	**1.0**	**1.1**	1.4	1.3	1.3
	6	1.8	1.9	2.0	**0.9**	0.8	0.8	1.7	1.8	1.3	1.3	1.2	1.6	1.4	1.8	**1.0**	1.3	**1.1**	1.1	1.3	1.4	1.4
	7	2.0	2.3	2.3	1.8	1.6	1.3	2.7	2.0	1.7	1.5	1.3	2.3	1.8	2.4	1.5	2.4	1.3	1.8	1.6	1.9	2.0
	8	0.8	1.4	1.3	0.7	**0.9**	**1.0**	1.3	**0.9**	0.8	0.8	**1.1**	**1.0**	0.8	1.2	**1.0**	0.7	**0.9**	1.2	1.2	**1.0**	0.8
	9	**0.9**	1.2	1.3	**1.0**	**1.1**	1.2	1.3	1.5	1.5	1.2	**0.9**	1.3	1.3	1.7	1.5	**0.9**	**1.1**	1.3	1.3	1.2	1.3
	10	**1.1**	**1.1**	**1.0**	**0.9**	0.8	1.4	**1.1**	**0.9**	**1.1**	**1.1**	**1.0**	**1.1**	1.2	1.6	1.3	1.2	**1.0**	1.3	**1.0**	**1.0**	1.2
	11	0.8	0.8	0.8	0.7	0.7	0.8	**0.9**	0.5	0.8	0.8	0.6	**1.0**	0.8	0.8	**0.9**	1.2	**0.9**	0.8	**0.9**	0.7	**0.9**
	12	0.8	0.8	0.7	**0.9**	**0.9**	**1.1**	0.7	0.8	0.7	0.7	**0.9**	**1.1**	**0.9**	0.8	**0.9**	1.3	1.4	0.7	**0.9**	0.8	**1.1**
Baytik station, 1580 m.a.s.l.	1	1.5	2.4	1.9	**1.1**	1.5	2.3	**1.1**	1.6	1.5	1.9	1.7	1.7	1.6	1.5	1.5	2.1	1.6	1.6	**1.1**	1.7	1.7
	2	**1.0**	1.2	**1.0**	0.8	**0.9**	1.4	**1.0**	**0.9**	0.7	**1.1**	**0.9**	1.2	0.7	**1.1**	0.6	1.3	1.2	0.9	**1.0**	**1.0**	**1.0**
	3	1.2	1.4	1.4	1.2	1.3	1.3	**1.1**	1.2	1.7	1.2	1.3	2.0	1.4	1.4	1.8	1.4	1.2	1.2	1.3	1.3	1.5
	4	**0.9**	1.3	**1.1**	**1.1**	0.7	1.3	0.8	0.8	**1.0**	1.3	0.8	**1.0**	1.2	**1.0**	**1.1**	1.2	0.8	0.5	**1.1**	**1.0**	**1.1**
	5	**1.1**	1.5	1.5	**0.9**	1.3	1.1	1.3	1.5	**1.1**	1.5	1.2	1.5	**0.9**	1.2	1.2	1.6	**1.0**	**1.0**	**1.0**	1.3	1.2
	6	1.5	1.6	1.7	0.7	0.7	0.7	1.5	1.6	**1.1**	**1.1**	**1.0**	1.3	1.2	1.5	0.8	**1.1**	**0.9**	**1.0**	**1.1**	1.2	**1.1**
	7	1.5	1.7	1.7	1.3	1.2	**0.9**	2.0	1.4	1.3	**1.1**	0.8	1.7	1.3	1.8	**1.1**	1.8	0.8	1.3	1.3	1.4	1.4
	8	0.8	1.4	1.2	0.7	**0.9**	**1.0**	1.3	0.8	0.7	0.8	1.2	**1.0**	0.8	1.2	**1.0**	0.7	0.8	1.2	1.2	**1.0**	**0.9**
	9	**1.1**	1.5	1.5	1.2	1.3	1.4	1.5	1.7	1.8	1.4	**1.1**	1.6	1.5	2.0	1.8	**1.1**	1.3	1.5	1.5	1.4	1.6
	10	**1.0**	**1.0**	**0.9**	0.8	0.7	1.2	**1.0**	0.8	**1.0**	**1.0**	**0.9**	**1.0**	**1.1**	1.5	1.2	1.2	**0.9**	1.2	**0.9**	**0.9**	1.2
	11	**0.9**	**0.9**	**0.9**	0.7	0.7	**0.9**	**1.0**	0.6	0.8	**0.9**	0.6	1.2	**0.9**	0.8	**1.0**	1.3	**1.0**	**0.9**	**0.9**	0.8	**1.0**
	12	0.8	0.8	0.7	**0.9**	**0.9**	**1.1**	0.7	0.8	0.7	0.7	0.8	**1.1**	0.8	0.8	**0.9**	1.2	1.4	0.6	**1.1**	0.8	**1.0**
Bishkek station, 756 m.a.s.l.	1	**1.1**	1.7	**1.0**	**1.0**	**1.1**	1.7	0.8	1.2	**1.0**	1.5	1.2	0.8	**1.1**	0.8	**1.1**	1.5	1.2	1.5	**0.9**	1.2	**1.1**
	2	0.8	**1.0**	0.7	0.8	0.7	1.2	0.8	0.8	0.6	**0.9**	0.7	0.7	0.8	0.8	**0.9**	**1.0**	**0.9**	0.8	**0.9**	0.8	**0.9**
	3	**1.1**	1.3	1.6	1.4	1.2	1.2	**1.0**	**1.1**	1.6	1.2	1.3	1.7	**1.1**	1.4	1.5	1.2	0.8	1.2	1.2	1.3	1.3
	4	**1.1**	1.3	**0.9**	**1.1**	0.8	1.3	0.8	**0.9**	1.2	**1.0**	0.8	**1.1**	1.3	**1.0**	**1.1**	1.3	0.8	0.7	**1.0**	**1.0**	**1.1**
	5	1.2	1.4	**1.0**	0.8	**1.1**	**1.0**	**1.1**	1.3	**1.0**	1.3	**1.1**	1.3	1.5	1.2	**0.9**	1.2	**1.0**	1.4	**1.1**	1.1	1.2
	6	1.6	1.6	0.8	0.7	0.7	0.7	1.5	1.6	**1.1**	**1.1**	**1.0**	1.8	**0.9**	1.5	0.8	1.3	0.8	**1.0**	1.6	1.1	1.2
	7	1.4	1.6	1.6	1.2	**1.1**	**0.9**	1.9	1.4	1.2	1.2	0.8	1.9	1.6	1.7	1.5	1.7	1.2	1.3	1.3	1.3	1.6
	8	**0.9**	1.4	0.7	0.8	**0.9**	1.2	1.4	**0.9**	0.8	**0.9**	**1.1**	**1.1**	**1.0**	1.3	1.3	0.7	1.2	1.4	1.2	**1.0**	**1.1**
	9	0.5	0.7	0.7	0.6	0.6	0.7	0.7	0.8	0.8	0.6	0.5	0.7	0.5	**0.9**	0.8	0.5	0.6	0.7	0.8	0.7	0.7
	10	**0.9**	**0.9**	0.7	0.7	0.7	**1.1**	0.8	0.7	**0.9**	**0.9**	0.8	**0.9**	0.8	1.3	**1.0**	**0.9**	0.7	1.2	**0.9**	0.8	**0.9**
	11	0.8	0.8	0.8	0.8	0.7	0.8	**0.9**	0.5	0.7	0.8	0.5	**0.9**	0.8	0.8	**1.1**	**1.0**	0.7	**0.9**	**1.0**	0.7	0.8
	12	0.6	0.6	0.8	**0.9**	0.7	0.8	0.5	0.6	0.5	0.5	0.7	0.6	0.6	**0.9**	**0.9**	0.8	**0.9**	0.7	**0.9**	0.7	0.8

The results of statistical analyses indicate that CMIP6 ACCESS-CM2, CORDEX REMO2015_HadGEM2-ES, and NHRCM-CA models performed best (rSD values close to 1) for both precipitation and temperature (Tables II and III, respectively). The multi-model ensembles (MMEs) show worse results than separate CMIP6 ACCESS-CM2 and CORDEX REMO2015_HadGEM2-ES models. Furthermore, the NHRCM-CA model performed best in precipitation simulations and replicated historical precipitation with $0.9 < rSD < 1.1$ over mountain and valley regions for all months except the summer period.

The three best model outputs are evaluated along with station observations; results of their BIAS (Fig. 5 and 6) show that NHRCM-CA still performs fairly well in simulating local climate. All simulated temperatures and precipitation exhibited high BIAS during summer (Fig. 5 and 6).

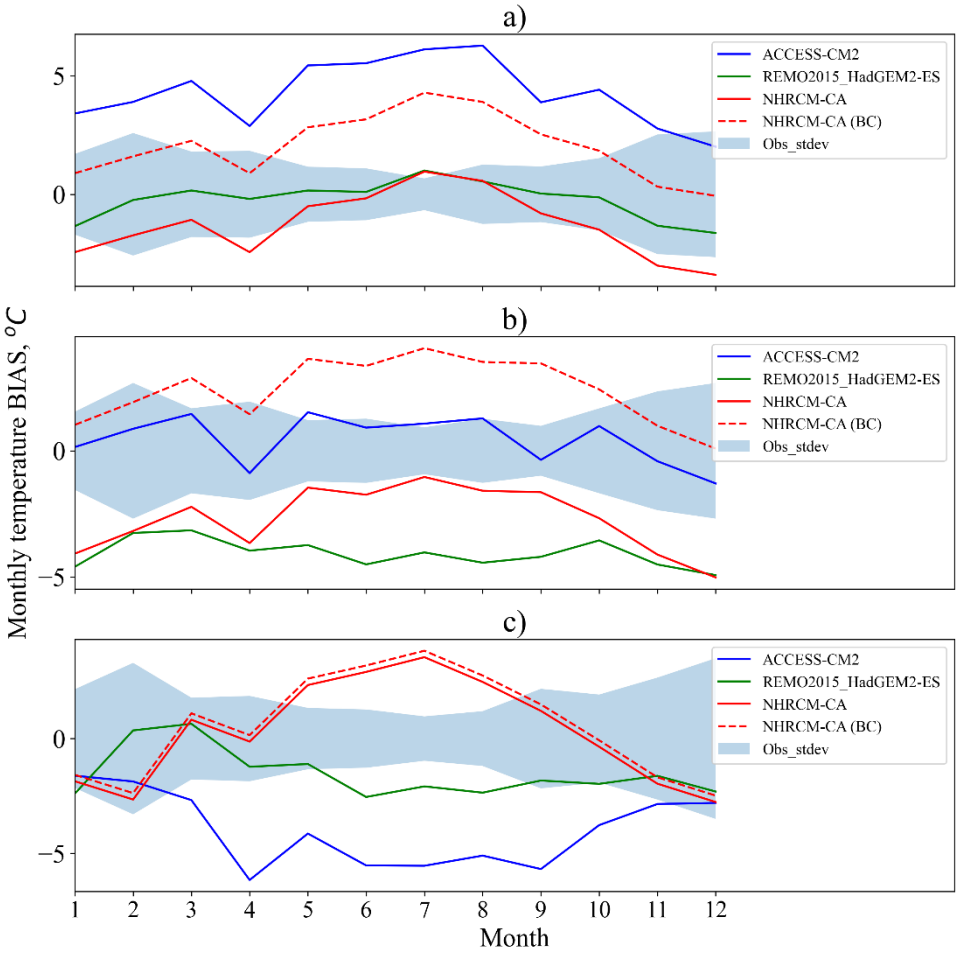

Figure 5. Comparisons among ACCESS-CM2, REMO2015_HadGEM2-ES, and NHRCM-CA monthly temperature BIAS at (a) Ala-Archa, (b) Baytik and (c) Bishkek meteorological stations for the period 1980-2000.

To reduce elevation difference between model grids and meteorological observation stations we incorporated a temperature lapse rate of 0.65 °C/100m multiplied by elevation difference. After elevation bias correction (BC) in high elevation station BIAS reduced (Fig. 5 a, b), but where the elevation difference was small there was no change (Fig. 5c).

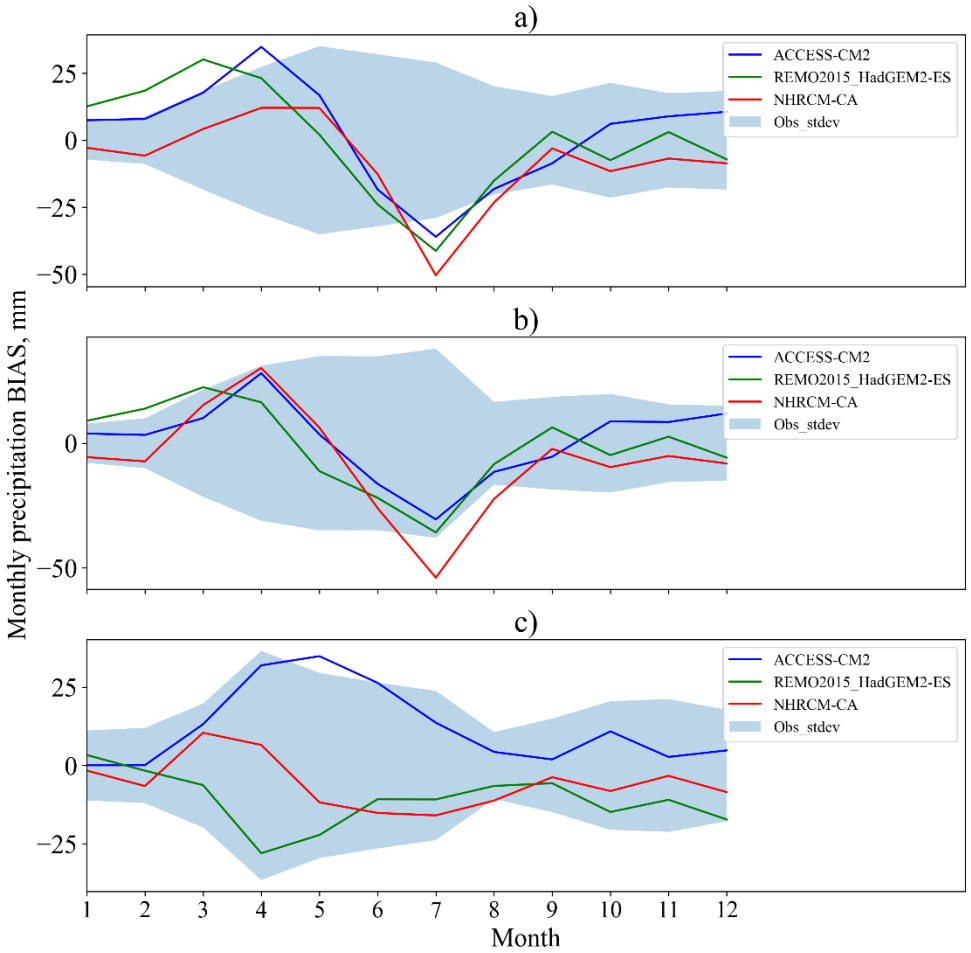

Figure 6. Comparisons between the ACCESS-CM2, REMO2015_HadGEM2-ES and NHRCM-CA monthly precipitation BIAS at (a) Ala-Archa, (b) Baytik and (c) Bishkek meteorological stations for period 1980-2000.

3.2. Projection of future climate change

All projected changes show the difference between means of future (2076–2096) and past (1980–2000) periods. Future changes of annual mean temperature (Fig. 7a) and precipitation (Fig. 7b) anomalies, and seasonal changes of temperature (Fig. 8) and precipitation (Fig. 9) anomalies during 2076–2096 across CA are derived from NHRCM-CA using the upper boundary SSP585 scenario with a base period of 1980-2000.

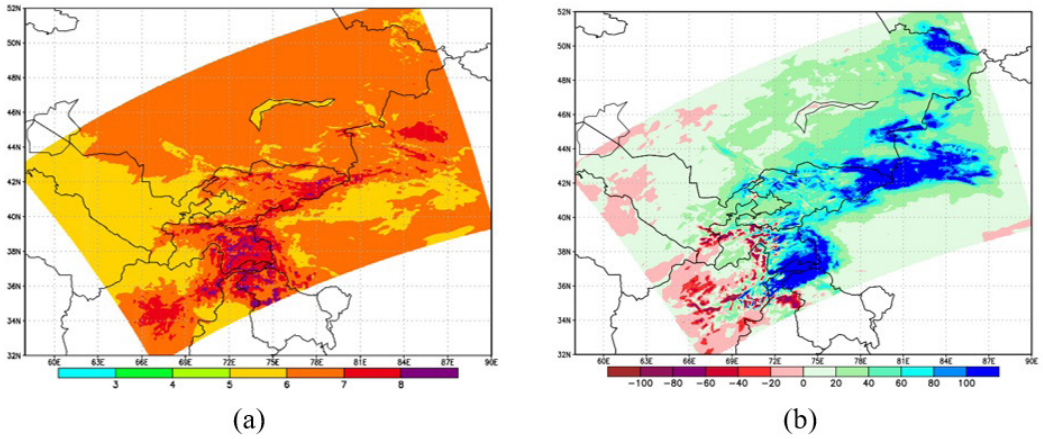

Figure 7. Future changes of annual mean temperature anomalies (°C) (a) and changes in annual precipitation totals (mm) (b) during 2076–2096 across CA derived from NHRCM-CA under the SSP585 scenario, base period: 1980-2000.

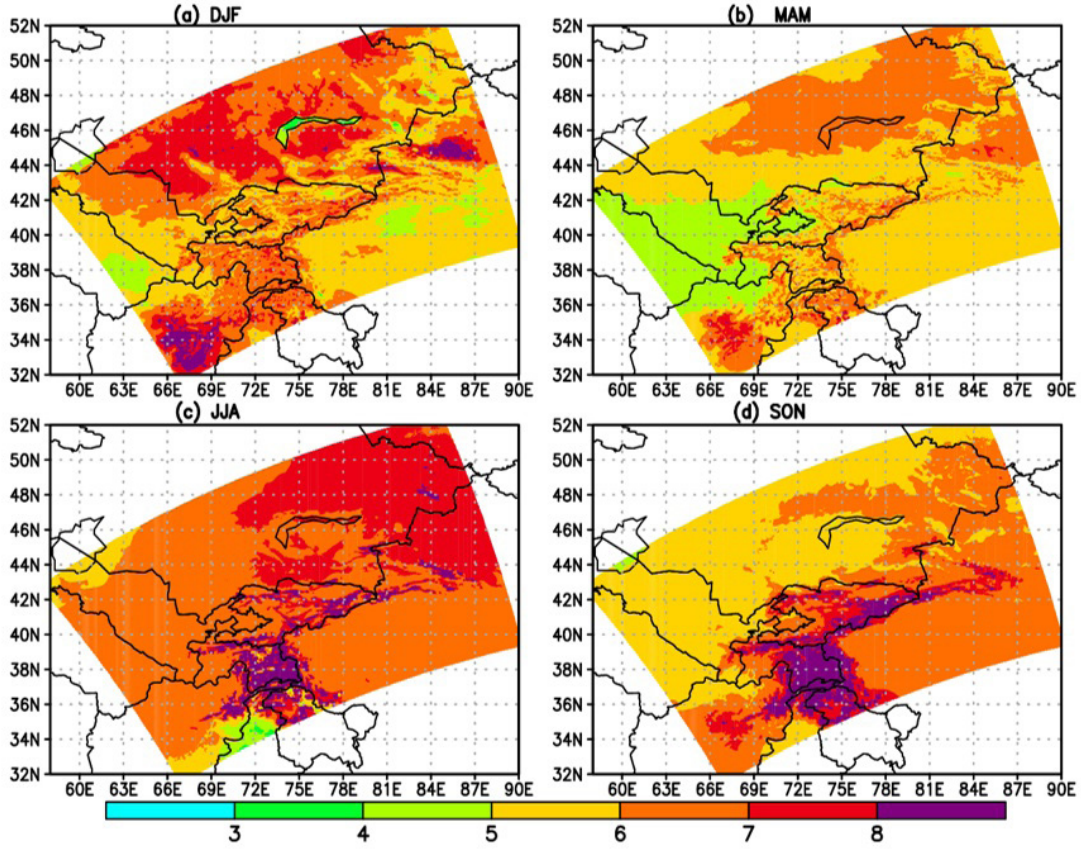

Figure 8. Future changes of seasonal mean temperature anomalies (°C) during 2076–2096 across CA derived from NHRCM-CA under SSP585 scenario, base period: 1980-2000; (a) winter; (b) spring; (c) summer; and (d) autumn.

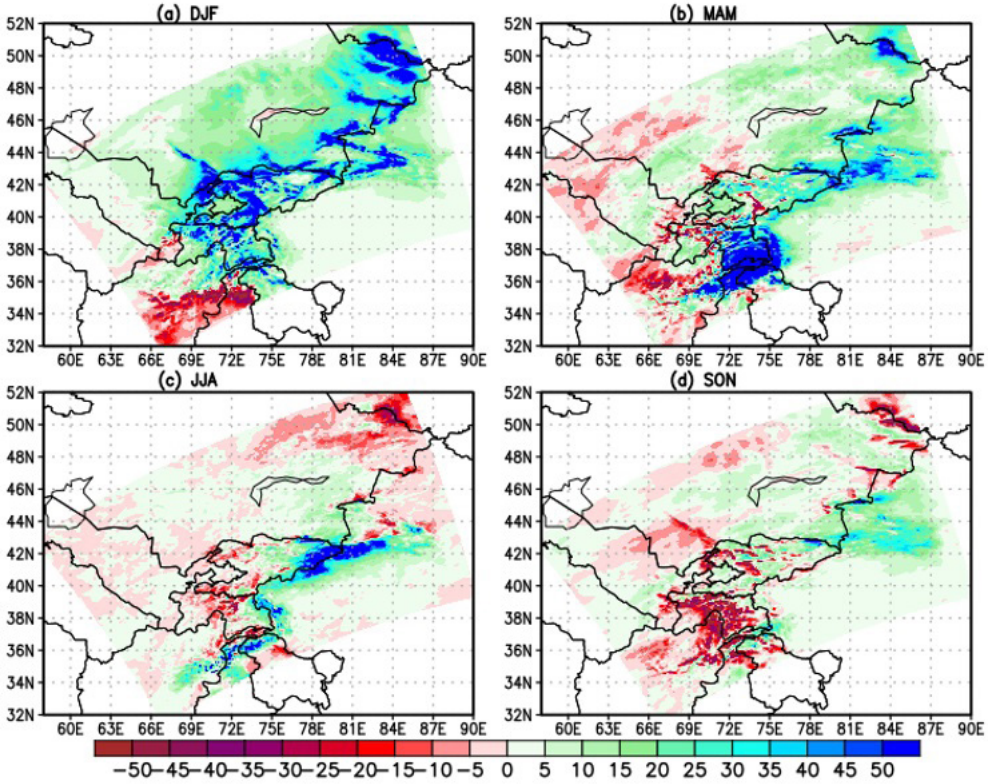

Figure 9. Future changes of seasonal precipitation anomalies (mm) during 2076–2096 across CA derived from NHRCM-CA under SSP585 scenario, base period: 1980-2000; (a) winter; (b) spring; (c) summer; and (d) autumn.

The NHRCM-CA model projects that annual mean temperature will increase by more than 6 °C in most of CA (Fig. 7 a). The projection under ssp5-8.5 shows that annual mean temperature (Fig. 7 a) and seasonal mean temperature (Fig. 8) will increase more significantly in the mountainous regions than the lower regions.

Annual precipitation is projected to increase mainly in two high-value regions in the Kyrgyzstan, Tajikistan, and northeast CA where the maximum simulated increase is from 60 mm to 100 mm (Fig. 7b). Annual precipitation declines will occur over northwest parts of Uzbekistan, Tajikistan and Afghanistan, with projected decreases from 5 mm to 20 mm by the end of this century (Fig. 7 b). The NHRCM-CA model projects precipitation increases from >5 mm to 35 mm in winter (Fig. 9 a) for the entire simulated domain except central Afghanistan where precipitation is expected to decrease by about 15 mm. In spring (Fig. 9 b), precipitation declines will occur over northwest Uzbekistan and Afghanistan, but increases are predicted over northeast Kazakhstan, Kyrgyzstan and Tajikistan. Projected summer precipitation declines across CA are >15 mm under SSP5-8.5 (Fig. 9c), except in northeast Kyrgyzstan,

Tajikistan and around Balkhash Lake in Kazakhstan. In autumn, precipitation (Fig. 9 d) will decline over Tajikistan, northern Afghanistan and the Shymkent region in Kazakhstan.

Projected future changes in monthly mean temperature and precipitation anomalies over major cities in CA derived from NHRCM-CA under the SSP585 scenario were estimated using 10,000 bootstrap samples with random replacement of the 20-yr dataset (significance level 5%) (Fig. 10 and 11). For all major CA cities, the projected monthly temperature increases by > 5 °C and all changes are statistically significant (Fig. 10). Statistically significant increases in projected monthly precipitation anomalies mostly occurred in spring and winter months for all major CA main cities (Fig. 11).

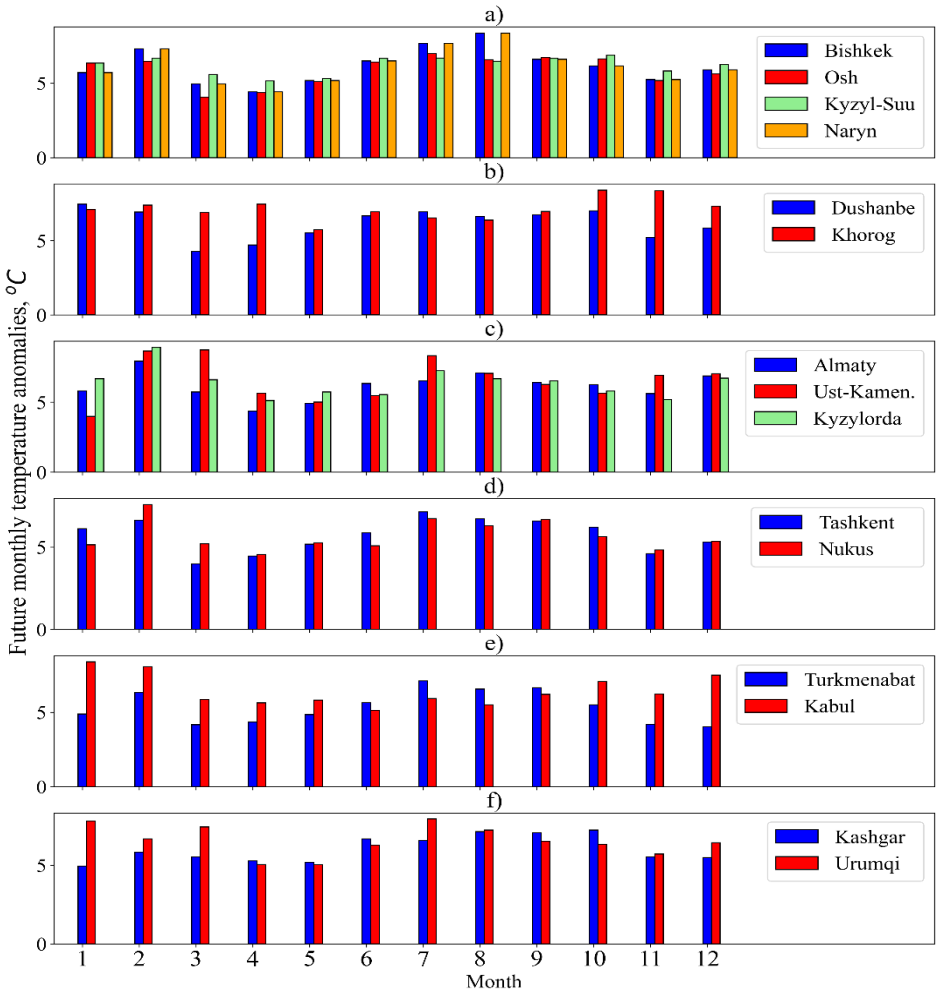

Figure 10. Future changes of monthly mean temperature anomalies (°C) during 2076–2096 over major CA cities derived from NHRCM-CA under the SSP585 scenario, base period: 1980-2000; cities in (a) Kyrgyzstan; (b) Tajikistan; (c) Kazakhstan; (d) Uzbekistan; (e) Turkmenistan and Afghanistan; and (f) nearby in China; all anomalies are statistically significant, p-level < 0.05 (estimated using 10,000 bootstrap samples with random replacement of the 20-yr dataset).

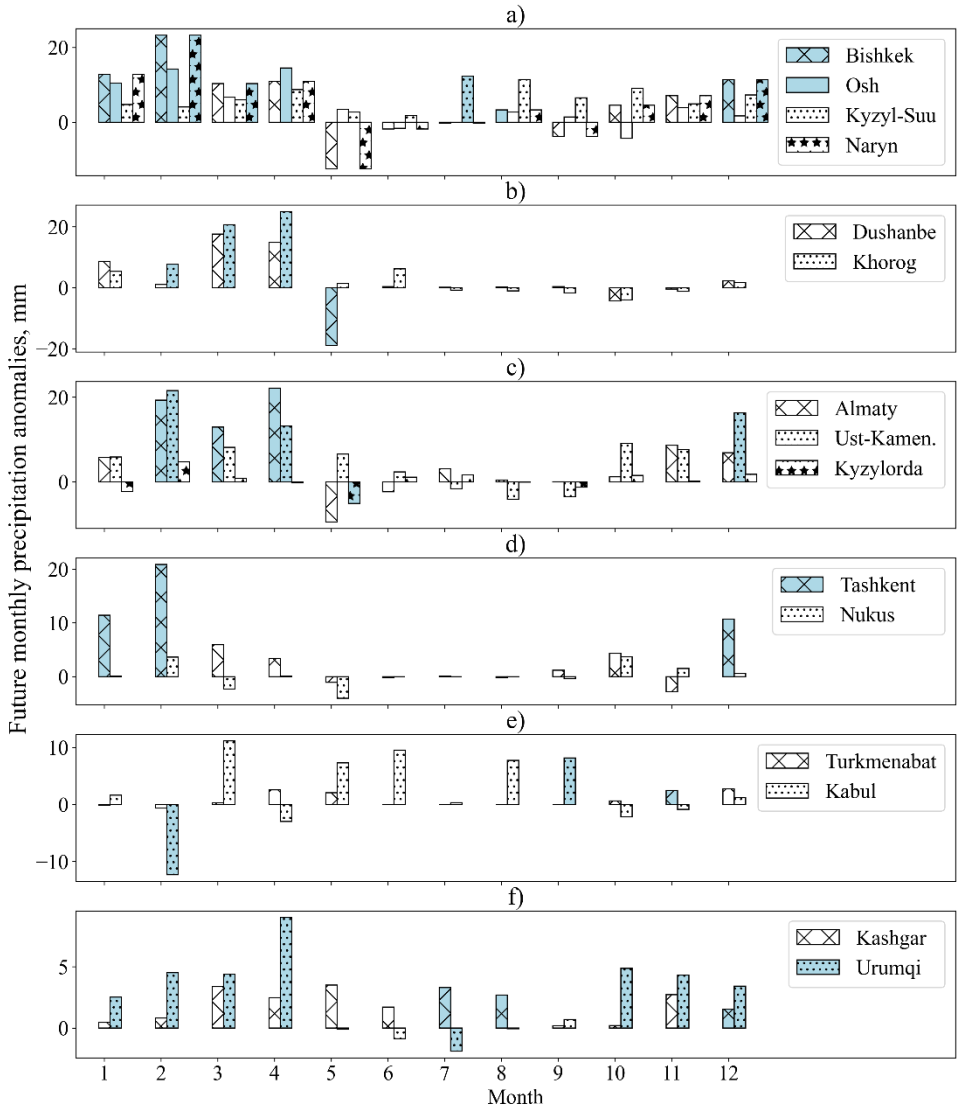

Figure 11. Future changes of monthly precipitation anomalies (mm) during 2076–2096 over major CA cities derived from NHRCM-CA under the SSP585 scenario, base period: 1980-2000; cities in (a) Kyrgyzstan; (b) Tajikistan; (c) Kazakhstan; (d) Uzbekistan;(e) Turkmenistan and Afghanistan; and (f) nearby in China; blue highlights indicate anomalies statistically significant, p-level < 0.05 (estimated using 10,000 bootstrap samples with random replacement of the 20-yr dataset).

4. Discussion and conclusions

The main goal of this research was to create a high-resolution (5 × 5 km) climate dataset across the mountainous region of CA for the period from 1980 to 2000 with climate projections in the period from 2076 to 2096. Such data are needed to develop sustainable climate change adaptation strategies in the region. To achieve

this goal, the NHRCM-CA model was used. Firstly, we evaluated the NHRCM-CA, GCM, and CORDEX-CAS RCMs simulations of temperature and precipitation. Results indicate that the high-resolution NHRCM-CA simulations better represent the local temperature and precipitation in CA, while significant systematic biases are present, especially in the mountainous areas. The dynamic downscaling of simulations of historical annual and seasonal precipitation and temperature over mountainous part of CA using NHRCM-CA show improvement compared with CMIP6 GCMs and CORDEX-CAS RCMs in terms of both climatological mean states and amplitudes of interannual variability. In particular, precipitation improved more than temperature. It can be explained by the advantages of using high-resolution RCM simulations such as better representation of topography and related meteorological fields over mountainous parts of CA. As mentioned in (Iles et al., 2020; Zeng et al., 2016), the resolution changes may strongly influence grid-scale structure of clouds and therefore precipitation. However, the RCM simulations still overestimate precipitation amounts over the mountainous areas of CA (Fig. 2b and Fig. 4). To address this issue, a convection-permitting resolution could be used (L.-L. Li et al., 2022), which suggests that all GCMs significantly overestimate precipitation over mountains and only with enhanced resolution can they provide more realistic fine-scale features of precipitation associated with local topography (Li et al., 2015).

As noted, MMEs are typically used to minimize GCM uncertainty and generate outputs consistent with local conditions. However, in regions with complex orography, using MMEs produced poor results (Tables II and III) because the averaging process also includes models with lower performance. In the absence of high-resolution regional models, and when GCMs must be used, it is better to select the best-performing models when calculating MMEs instead of averaging all GCMs. Further improvements in climate simulations can be considered through the implementation of statistical or machine learning-based bias correction methods (Isaev, Ermanova, et al., 2022; Iturbide et al., 2019).

Results of the dynamic downscaling experiments with NHRCM-CA show that annual and seasonal temperatures across CA will rise significantly in the future with increases concentrated mostly in mountainous regions. Simulations indicate that significant warming will occur across CA with a projected increase of 6°C under SSP5-8.5 from 2076 to 2096. Temperature will increase significantly if greenhouse gas emissions significantly increase, especially in summer. Therefore, controlling greenhouse gas emissions is a priority for mitigating warming. Pronounced warming is detected over mountainous areas of CA from autumn to spring, which can be explained by the snow-albedo feedback.

Projected temperature increases (Fig. 8 c) in summer will increase the intensity and frequency of droughts, which may exacerbate cross-border conflicts related to water supplies in CA (Wang et al., 2021). Projected temperature and precipitation increases in winter and spring may increase climate-related hazards such as snow avalanches and landslides. Flood hazards may also increase with increasing rainfall and temperature, the latter causing rapid snowmelt. Much of the precipitation during winter and spring is related to synoptic processes, such as the South Caspian cyclone, Murgab cyclone, Upper Amu River cyclone, Northwest invasion, and Western invasion over CA (Isaev, Ajikeev, et al., 2022). In relation to the projections, precipitation shows an increase during spring and winter, suggesting that these synoptic processes might intensify during those seasons.

As mentioned previously, the effectiveness of the high-resolution downscaling method for temperature and precipitation at regional and local scales will bring advantages to research areas of climate change adaptation in CA. Abundant daily observation data for CA are required for model validation, which is a challenge in this region. Our results demonstrated that a high-resolution RCM was a useful tool to project local-scale changes in temperature and precipitation. Nevertheless, significant uncertainties remain in dynamic downscaling simulations, affecting the credibility of future climate change projections. The most effective way to reduce these uncertainties is downscaling multi-models and their ensembles. However, our results were based on a single model due to the fine model resolution because it was difficult to conduct ensemble simulations with our available computing resources. Furthermore, the limitations of the current study include the utilization of only three in-situ observations. Future research should prioritize ensemble simulations to assess uncertainties stemming from various error sources, such as truncation errors, model boundary conditions, and parametrization errors associated with physical processes. Additionally, expanding the number of observations would enable more comprehensive verification across the study region.

Acknowledgments

The authors thank Dr. Ryo Mizuta of Meteorological Research Institute for providing the AGCM data: The boundary conditions for NHRCM.

Author Contributions: Conceptualization, E.I. and A.M.; methodology, A.M. and E.I; software, Sh.F. and E.I.; validation, E.I., A.M., R.C.S. and Sh.F.; resources, A.M. writing—original draft preparation, E.I.; writing—review and editing, R.C.S. and E.I. All authors have read and agreed to the published version of the manuscript.

Funding: This work was supported by MEXT-Program for the advanced studies of climate change projection (SENTAN) Grant Number JPMXD0722680734. This work

was also supported under The United Nations General Assembly declaration the year 2022 as the International Year of Sustainable Mountain Development (document A/76/L.28), at the proposal of the Government of the Kyrgyz Republic.

References

Aitaliev, A., Sakyev, D., Nazarkulov, K., Amanova, M., Brejneva, V., Spektorenko, N., Aidaraliev, N., Sataev, S., Jumanazarov, A., & Ymanbekov, K. (2020). Atlas of natural and man-made hazards on the territory of the Kyrgyz Republic. *Ministry Emergency Situations Ministry*. Kyrgyz Republic. https://mchs.gov.kg/ru/atlas/

Alexander, L. V., Zhang, X., Peterson, T. C., Caesar, J., Gleason, B., Klein Tank, A. M. G., Haylock, M., Collins, D., Trewin, B., Rahimzadeh, F., Tagipour, A., Rupa Kumar, K., Revadekar, J., Griffiths, G., Vincent, L., Stephenson, D. B., Burn, J., Aguilar, E., Brunet, M., … Vazquez-Aguirre, J. L. (2006). Global observed changes in daily climate extremes of temperature and precipitation. *Journal of Geophysical Research: Atmospheres*, 111(D5), 5109. https://doi.org/10.1029/2005JD006290

Bernauer, T., & Siegfried, T. (2012). Climate change and international water conflict in Central Asia. Http://Dx.Doi.Org/10.1177/0022343311425843, 49(1), 227–239. https://doi.org/10.1177/0022343311425843

Bruyère, C. L., Done, J. M., Holland, G. J., & Fredrick, S. (2014). Bias corrections of global models for regional climate simulations of high-impact weather. *Climate Dynamics*, 43, 1847–1856. https://doi.org/10.1007/s00382-013-2011-6

Chang, S., Isaev, E., Chen, H., Wu, B., Meng, J., Yan, N., & Ma, Z. (2024). Exploring the Linkages between Different Types of Drought and Their Impacts on Crop Production in Kyrgyzstan. *IEEE Journal of Selected Topics in Applied Earth Observations and Remote Sensing*. https://doi.org/10.1109/JSTARS.2024.3359429

CHIRPS: Rainfall Estimates from Rain Gauge and Satellite Observations | Climate Hazards Center - UC Santa Barbara. (2022). https://www.chc.ucsb.edu/data/chirps

CMIP5 Data Search | CMIP5 | ESGF-CoG. (2022). https://esgf-node.llnl.gov/search/cmip5/

cmip6 Data Search | cmip6 | ESGF-CoG. (2022). https://esgf-node.llnl.gov/search/cmip6/

CORDEX-DKRZ Data Search | CORDEX-DKRZ | ESGF-CoG. (2022). https://esgf-data.dkrz.de/search/cordex-dkrz/

Funk, C., Peterson, P., Landsfeld, M., Pedreros, D., Verdin, J., Shukla, S., Husak, G., Rowland, J., Harrison, L., Hoell, A., & Michaelsen, J. (2015). The climate hazards infrared precipitation with stations—a new environmental record for monitoring extremes. *Scientific Data 2015 2:1*, 2(1), 1–21. https://doi.org/10.1038/sdata.2015.66

Gulakhmadov, A., Chen, X., Gulahmadov, N., Liu, T., Anjum, M. N., & Rizwan, M. (2020). Simulation of the Potential Impacts of Projected Climate Change on Streamflow in the Vakhsh River Basin in Central Asia under CMIP5 RCP Scenarios. *Water*, Vol. 12, Page 1426, 12(5), 1426. https://doi.org/10.3390/W12051426

Harris, I., Osborn, T. J., Jones, P., & Lister, D. (2020). Version 4 of the CRU TS monthly high-resolution gridded multivariate climate dataset. *Scientific Data, 7:1*, 7(1), 1–18. https://doi.org/10.1038/s41597-020-0453-3

Hirai, M., & Oh'izumi, M. (2004). Development of a new landsurface model for JMA-GSM. Development of a New Landsurface Model for JMA-GSM. *Extended Abstract of 20th Conference on Weather Analysis and Forecasting/16th Conference on NWP*. P2.22.

Huang, A., Zhou, Y., Zhang, Y., Huang, D., Zhao, Y., & Wu, H. (2014). Changes of the annual precipitation over central Asia in the twenty-first century projected by multimodels of CMIP5. *Journal of Climate*, 27(17), 6627–6646. https://doi.org/10.1175/JCLI-D-14-00070.1

Iles, C. E., Vautard, R., Strachan, J., Joussaume, S., Eggen, B. R., & Hewitt, C. D. (2020). The benefits of increasing resolution in global and regional climate simulations for European climate extremes. *Geoscientific Model Development*, 13(11), 5583–5607. https://doi.org/10.5194/GMD-13-5583-2020

Immerzeel, W. W., Van Beek, L. P. H., & Bierkens, M. F. P. (2010). Climate change will affect the asian water towers. *Science*, 328(5984), 1382–1385. https://doi.org/10.1126/SCIENCE.1183188/SUPPL_FILE/IMMERZEEL.SOM.PDF

Isaev, E., Ajikeev, B., Shamyrkanov, U., Kalnur, K., Maisalbek, K., & Sidle, R. C. (2022). Impact of Climate Change and Air Pollution Forecasting Using Machine Learning Techniques in Bishkek. *Aerosol and Air Quality Research*, 22(3), 210336. https://doi.org/10.4209/AAQR.210336

Isaev, E., Ermanova, M., Sidle, R. C., Zaginaev, V., Kulikov, M., & Chontoev, D. (2022). Reconstruction of Hydrometeorological Data Using Dendrochronology and Machine Learning Approaches to Bias-Correct Climate Models in Northern Tien Shan, Kyrgyzstan. *Water*, 14(15), 2297. https://doi.org/10.3390/W14152297

Isaev, E. K., Aniskina, O. G., & Mostamandi, S. V. (2017). Investigation of sensitivity of the hydrodynamic modeling in an area with difficult terrain to the parameters of the planetary boundary layer. *Works of Voeikov Main Geophysical Observatory,* 584, 123–142. https://www.researchgate.net/publication/339042796_Investigation_of_sensitivity_of_the_hydrodynamic_modeling_in_an_area_with_difficult_terrain_to_the_parameters_of_the_planetary_boundary_layer

Isaev, E., Kulikov, M., Shibkov, E., & Sidle, R. C. (2022). Bias correction of Sentinel-2 with unmanned aerial vehicle multispectral data for use in monitoring walnut fruit forest in western Tien Shan, Kyrgyzstan. Https://Doi.Org/10.1117/1.JRS.17.022204, 17(2), 022204. https://doi.org/10.1117/1.JRS.17.022204

Isaev, E., & Omurzakova, S. (2019). On the possibility of drought detection and modeling in Kyrgyzstan. *Bulletin of the Kyrgyz- Russian Slavic University*, 11, 172–176. (in Russian)

Iturbide, M., Bedia, J., Herrera, S., Baño-Medina, J., Fernández, J., Frías, M. D., Manzanas, R., San-Martín, D., Cimadevilla, E., Cofiño, A. S., & Gutiérrez, J. M. (2019). The R-based climate4R open framework for reproducible climate data access and post-processing. *Environmental Modelling & Software,* 111, 2–54. https://doi.org/https://doi.org/10.1016/j.envsoft.2018.09.009

Jiang, J., Zhou, T., Chen, X., & Zhang, L. (2020). Future changes in precipitation over Central Asia based on CMIP6 projections. *Environmental Research Letters*, 15(5). https://doi.org/10.1088/1748-9326/AB7D03

Kain, J., & Fritsch, M. (1990). A One-Dimensional Entraining/Detraining Plume Model and Its Application in Convective Parameterization . *Journal of the Atmospheric Sciences*, 47(23), 2784–2802. https://journals.ametsoc.org/view/journals/atsc/47/23/1520-0469_1990_047_2784_aodepm_2_0_co_2.xml

Kaplina, A., Olofinskaya, N., Kozomara, M., & Mills Janine, Twymanand Selenge, S. (2018). Climate Change adaptation in Europe and Central asia: Adapting to a changing climate for resilient development. https://www.adaptation-undp.org/sites/default/files/resources/climate_change_adaptation_in_europe_and_central_asia.pdf

Kastridis, A., Stathis, D., Sapountzis, M., & Theodosiou, G. (2022). Insect Outbreak and Long-Term Post-Fire Effects on Soil Erosion in Mediterranean Suburban Forest. *Land*, Vol. 11, Page 911, 11(6), 911. https://doi.org/10.3390/LAND11060911

Kida, H., Koide, T., Sasaki, H., & Chiba, M. (1991). A new approach to coupling a limited area model with a GCM for regional climate simulations. J. Meteor. Soc. *Japan*, 69, 723–728.

Kitagawa, H. (2000). Radiation processes. *Separate Volume of Annual Report of NPD*, 46, 16-31 (in Japanese).

Li, J., Yu, R., Yuan, W., Chen, H., Sun, W., & Zhang, Y. (2015). Precipitation over East Asia simulated by NCAR CAM5 at different horizontal resolutions. J. *Adv. Model. Earth Syst.*, 7, 774–790. https://doi.org/10.1002/2014MS000414

Li, L.-L., Li, J., & Yu, R. (2022). Evaluation of CMIP6 HighResMIP models in simulating precipitation over Central Asia. *Advances in Climate Change Research*, 13(1), 1–13. https://doi.org/https://doi.org/10.1016/j.accre.2021.09.009

Lin, Y. H., & Farley, R. D. (1983). Bulk parameterization of the snow field in a cloud model. *J.Clim. Appl. Meteor.*, 22, 1065–1092.

Luo, Y., Wang, X., Piao, S., Sun, L., Ciais, P., Zhang, Y., Ma, C., Gan, R., & He, C. (2018). Contrasting streamflow regimes induced by melting glaciers across the Tien Shan – Pamir – North Karakoram. *Scientific Reports* 8:1, 8(1), 1–9. https://doi.org/10.1038/s41598-018-34829-2

Manandhar, S., Xenarios, S., Schmidt-Vogt, D., Hergarten, C., & Foggin, M. (2018). Climate Vulnerability & Adaptive Capacity of Mountain Societies in Central Asia. https://ucentralasia.org/media/wygpwq22/web-no3-msri-research-paper.pdf

Mizuta, R., Yoshimura, H., Murakami, H., Matsueda, M., Endo, H., Ose, T., Kamiguchi, K., Hosaka, M., Sugi, M., Yukimoto, S., Kusunoki, S., & Kitoh, A. (2012). Climate Simulations Using MRI-AGCM3.2 with 20-km Grid. Journal of the Meteorological Society of Japan. *Ser. II*, 90A(A), 233–258. https://doi.org/10.2151/JMSJ.2012-A12

Murata, A., Sasaki, H., Kawase, H., & Nosaka, M. (2016). Evaluation of precipitation over an oceanic region of Japan in convection-permitting regional climate model simulations. *Climate Dynamics 48:5*, 48(5), 1779–1792. https://doi.org/10.1007/S00382-016-3172-X

Murata, A., Sasaki, H., Kawase, H., Nosaka, M., Aoyagi, T., Oh'izumi, M., Seino, N., Shido, F., Hibino, K., Ishihara, K., Murai, H., Yasui, S., Wakamatsu, S., & Takayabu, I. (2017). Projection of Future Climate Change over Japan in Ensemble Simulations Using a Convection-Permitting Regional Climate Model with Urban Canopy. *SOLA*, 13, 219–223. https://doi.org/10.2151/SOLA.2017-040

Muratalieva, N. (2022). Climate change in CA. CABAR.Asia. https://cabar.asia/ru/izmenenie-klimata-v-tsentralnoj-azii-tochka-nevozvrata-projdena

Nakanishi, M., & Niino, H. (2004). An improved Mellor–Yamada level-3 model with condensation physics: Its design and verification. Bound. *Layer Meteor.*, 112, 1–31.

Nakano, M., Kato, T., Hayashi, S., Kanada, S., Yamada, Y., & Kurihara, K. (2012). Development of a 5-km-Mesh Cloud-System-Resolving Regional Climate Model at the Meteorological Research Institute. *Journal of the Meteorological Society of Japan*. Ser. II, 90A(A), 339–350. https://doi.org/10.2151/JMSJ.2012-A19

Nowak, A., Nowak, S., Nobis, M., & Nobis, A. (2016). Vegetation of screes of the montane and colline zones in the Pamir-Alai Mts in Tajikistan (Middle Asia). *Tuexenia*, 36, 223–248. https://doi.org/10.14471/2016.36.001

Oh'izumi, M. (2014). Introduction of PBL schemes to iSiB submodel in NHRCM. Proc. of the Fall Conference of Meteor. Soc. of Japan, 172. (in Japanese)

Ozturk, T., Turp, M. T., Türkeş, M., & Kurnaz, M. L. (2017). Projected changes in temperature and precipitation climatology of Central Asia CORDEX Region 8 by using RegCM4.3.5. *Atmospheric Research*, 183, 296–307. https://doi.org/10.1016/J.ATMOSRES.2016.09.008

Pachauri, R.K., Meyer, L. A. (2014). IPCC. Climate Change 2014: Synthesis Report. Contribution of Working Groups I, II, and III to the Fifth Assessment Report of the Intergovernmental Panel on Climate Change;

Park, S., Lim, C. H., Kim, S. J., Isaev, E., Choi, S. E., Lee, S. D., & Lee, W. K. (2021). Assessing climate change impact on cropland suitability in kyrgyzstan: Where are potential high-quality cropland and the way to the future. *Agronomy*, 11(8). https://doi.org/10.3390/AGRONOMY11081490

Qiu, Y., Feng, J., Yan, Z., Wang, J., & Li, Z. (2021). High-resolution dynamical downscaling for regional climate projection in Central Asia based on bias-corrected multiple GCMs. *Climate Dynamics 58:3*, 58(3), 777–791. https://doi.org/10.1007/S00382-021-05934-2

Qiu, Y., Hu, Q., & Zhang, C. (2017). WRF simulation and downscaling of local climate in Central Asia. *International Journal of Climatology*, 37, 513–528. https://doi.org/10.1002/JOC.5018

Rasmussen, R., Liu, C., Ikeda, K., Gochis, D., Yates, D., Chen, F., Tewari, M., Barlage, M., Dudhia, J., Yu, W., Miller, K., Arsenault, K., Grubišić, V., Thompson, G., & Gutmann, E. (2011). High-Resolution Coupled Climate Runoff Simulations of Seasonal Snowfall over Colorado: A Process Study of Current and Warmer Climate. *Journal of Climate*, 24(12), 3015–3048. https://doi.org/10.1175/2010JCLI3985.1

Russo, E., Kirchner, I., Pfahl, S., Schaap, M., & Cubasch, U. (2019). Sensitivity studies with the regional climate model COSMO-CLM 5.0 over the CORDEX Central Asia Domain. *Geoscientific Model Development,* 12(12), 5229–5249. https://doi.org/10.5194/GMD-12-5229-2019

Russo, E., Lund Sørland, S., Kirchner, I., Schaap, M., Raible, C. C., & Cubasch, U. (2020). Exploring the parameter space of the COSMO-CLM v5.0 regional climate model for the Central Asia CORDEX domain. *Geoscientific Model Development*, 13(11), 5779–5797. https://doi.org/10.5194/GMD-13-5779-2020

Saito, K., Fujita, T., Yamada, Y., Ishida, J. I., Kumagai, Y., Aranami, K., Ohmori, S., Nagasawa, R., Kumagai, S., Muroi, C., Kato, T., Eito, H., & Yamazaki, Y. (2006). The Operational JMA Nonhydrostatic Mesoscale Model. *Monthly Weather Review*, 134(4), 1266–1298. https://doi.org/10.1175/MWR3120.1

Saito, K., Ishida, J. I., Aranami, K., Hara, T., Segawa, T., Narita, M., & Honda, Y. (2007). Nonhydrostatic Atmospheric Models and Operational Development at JMA. *Journal of the Meteorological Society of Japan*. Ser. II, 85B, 271–304. https://doi.org/10.2151/JMSJ.85B.271

Sasaki, H., Kurihara, K., Takayabu, I., & Uchiyama, T. (2008). Preliminary Experiments of Reproducing the Present Climate Using the Non-hydrostatic Regional Climate Model. *SOLA*, 4, 25–28. https://doi.org/10.2151/SOLA.2008-007

Sasaki, H., Sato, Y., Adachi, K., & Kida, H. (2000). Performance and evaluation of the MRI regional climate model with the spectral boundary coupling method. *J. Meteor. Soc. Japan*, 78, 477–489.

Sillmann, J., Kharin, V. V., Zwiers, F. W., Zhang, X., & Bronaugh, D. (2013). Climate extremes indices in the CMIP5 multimodel ensemble: Part 2. Future climate projections. *Journal of Geophysical Research: Atmospheres*, 118(6), 2473–2493. https://doi.org/10.1002/JGRD.50188

Ta, Z., Yu, Y., Sun, L., Chen, X., Mu, G., & Yu, R. (2018). Assessment of precipitation simulations in Central Asia by CMIP5 climate models. *Water (Switzerland)*, 10(11). https://doi.org/10.3390/W10111516

Vakulchuk, R., Daloz, A. S., Overland, I., Sagbakken, H. F., & Standal, K. (2022). A void in Central Asia research: climate change. Https://Doi.Org/10.1080/02634937.2022.2059447, 1–20. https://doi.org/10.1080/02634937.2022.2059447

Wang, Q., Yi, S., & Sun, W. (2017). Precipitation-driven glacier changes in the Pamir and Hindu Kush mountains. *Geophysical Research Letters*, 44(6), 2817–2824. https://doi.org/10.1002/2017GL072646

Wang, X., Chen, Y., Li, Z., Fang, G., Wang, F., & Hao, H. (2021). Water resources management and dynamic changes in water politics in the transboundary river basins of Central Asia. *Hydrol. Earth Syst. Sci.*, 25, 3281–3299. https://doi.org/https://doi.org/10.5194/hess-25-3281-2021

Wang, Y., Feng, J., Luo, M., Wang, J., & Qiu, Y. (2020). Uncertainties in simulating central Asia: Sensitivity to physical parameterizations using Weather Research and Forecasting model. *International Journal of Climatology,* 40(14), 5813–5828. https://doi.org/10.1002/JOC.6567

Wehner, M. (2013). Methods of projecting future changes in extremes. *Water Sci. Technol. Libr.*, 65, 223–237.

Yabu, S., Murai, S., & Kitagawa, H. (2005). Clear sky radiation scheme. *Separate Volume of Annual Report of NPD*, 51, 53-64 (in Japanese).

Yonehara, H., Tokuhiro, T., Nagasawa, R., Ujiie, M., Shimokobe, A., Nakagawa, M., Sekiguchi, R., Kanehama, T., Sato, H., & Saito, K. (2017). Upgrade of parameterization schemes in JMA's operational global NWP model. In WGNE Research Activities in Atmospheric and Oceanic Modelling (pp. 17–18). CAS/JSC Working Group on Numerical Experimentation.

Zeng, X. M., Wang, M., Zhang, Y., Wang, Y., & Zheng, Y. (2016). Assessing the Effects of Spatial Resolution on Regional Climate Model Simulated Summer Temperature and Precipitation in China: A Case Study. *Advances in Meteorology*. https://doi.org/10.1155/2016/7639567

Zhu, X., Wei, Z., Dong, W., Ji, Z., Wen, X., Zheng, Z., Yan, D., & Chen, D. (2020). Dynamical downscaling simulation and projection for mean and extreme temperature and precipitation over central Asia. *Climate Dynamics*, 54(7–8), 3279–3306. https://doi.org/10.1007/S00382-020-05170-0